Detecting Hydrogen in Helium Streams

Samuel Goodman

Pittsford Mendon High School

Rochester, New York

Advisor: Dr. Walter Shmayda

Laboratory for Laser Energetics

University of Rochester

Rochester, New York

September 2013

Abstract

Three different approaches to detecting hydrogen in helium streams were assessed: thermal conductivity, atmospheric sampling using a mass spectrometer, and permeation through a palladium/silver membrane. The thermal conductivity detection system utilized an assembly of four cells fitted with filaments wired to make a Wheatstone bridge. Pure helium flowed through two of the cells. Helium containing hydrogen passed through the remaining two cells. The filament temperature, which is determined by the thermal conductivity of the gas surrounding the filaments, depends on the hydrogen concentration in the helium carrier. In the atmospheric sampling approach, a slip-stream is drawn from the carrier via two differentially pumped orifices and injected into a vacuum system. The vacuum system is fitted with a mass spectrometer tuned to hydrogen. In the permeation approach, the helium stream is passed over a hot palladium/silver (Pd/Ag) membrane. Hydrogen permeates through the membrane to increase the pressure in a vacuum system. The change in the vacuum pressure is directly related to the hydrogen concentration in the carrier on the upstream side of the membrane. The Pd/Ag permeation approach proved to be the most sensitive hydrogen detection technique. This approach was used to investigate the performance of a cryotrap. Several interesting phenomena were detected when evaluating the cryotrap. A large but brief breakthrough occurs when the column reaches capacity, and hydrogen elution can occur when the full, cold column is purged with helium.

Introduction

The University of Rochester Laboratory for Laser Energetics (LLE), whilst carrying out internal confinement fusion experiments, utilizes tritium gas, one of the reactants required for the fusion process, in the fabrication of its cryogenic targets. Tritium processing equipment is typically encased in a glovebox to prevent the release of the tritium to the environment. Helium is used as a purge gas in the glovebox. Any tritium that has been released from process equipment is swept out of the glovebox and collected by zirconium-iron (ZrFe) alloy. Annually, the ZrFe alloy is removed from the box circulation loop to recover the tritium. Tritium is released from the alloy into a helium carrier stream by heating the ZrFe to 450° C. One proposed method for recovering the tritium from this inert gas stream is a cryotrap.**(1)**

The cryotrap is a specialized coil of stainless steel tubing filled with a molecular sieve. The helium containing tritium is flown through the cryotrap. When cooled to liquid nitrogen temperatures (77 K), the molecular sieve extracts tritium from the carrier stream, while helium flows out the other end of the cryotrap. When the temperature of the molecular sieve is raised above liquid nitrogen temperatures, tritium is released back into the carrier stream and exits the cryotrap. This way, tritium can be concentrated and recovered, minimizing risk and emissions.

To evaluate the cryotrap’s ability to collect, store and release tritium, three systems for detecting hydrogen in a helium stream were proposed, constructed, and calibrated. For the sake of safety and convenience, tritium was replaced with hydrogen for all experiments, as its behavior is almost identical when interacting with the molecular sieve, the vacuum-backed membrane, and various detectors. The most sensitive system was then used to investigate the performance of the cryotrap.

System 1

The first detection system relied on a thermal conductivity detector (TCD). The TCD consists of four cells: two are used as reference, while the other two are used for the sample itself. These cells are aligned in a Wheatstone bridge configuration (figure 1). Hydrogen gas flows through the sample cells in a helium carrier, while the reference cells are exposed to pure helium gas. When the concentration of hydrogen in helium changes through the sample cells, the thermal conductivity of the gas stream changes, causing a change in temperature of the cell's filament.(2) This temperature change results in a changed resistance in the circuit shown in figure 1. The resistance change results in a different voltage output from the TCD. The Wheatstone bridge is balanced when gas compositions across all reference and sample cells are the same. When this occurs, the voltage output is zero.

This hydrogen detection system proved problematic. The thermal conductivities of hydrogen and helium are very similar, 0.1805 $W \cdot m^{-1} \cdot K^{-1}$ for hydrogen compared to 0.1513 $W \cdot m^{-1} \cdot K^{-1}$ for helium. Because the sample gas stream was primarily composed of helium, with the hydrogen concentration often less than 2% of the helium concentration, the signal-to-noise ratio of the TCD voltage output was low, regardless of the differences in gas flow rate and hydrogen concentration. The TCD was operated at temperatures ranging from 80° C to 200° C in an attempt to enhance the TCD's response relative to the helium carrier, but no significant difference in the signal-to-noise ratio was produced. Shielded cabling also failed to significantly reduce noise.

Options to improve hydrogen detectability include a more sensitive TCD, the implementation of a lock-in amplifier, or the use of an inert carrier gas with a thermal conductivity more remote from that of hydrogen.

System 2

The second proposed system relies on an atmospheric sampling system with an RF-quadrupole mass spectrometer. The schematic for this system can be found in figure 2. Gas flow is initially regulated by two mass flow controllers (MFCs). The slip stream of the carrier gas is pumped through a precision micro-orifice. The delivery pressure of the hydrogen/helium slip stream is measured by the first ion gauge P_1. From there, a sample stream passes through a second precision micro-orifice (leftward of P_1 in figure 2) and into the vacuum chamber created by the turbomolecular pump. The pressure of the sample stream is measured by the second ion gauge P_2, and the pressures of the individual molecular components of the sample stream are measured by the RF-quadrupole within the residual gas analyzer (RGA). The flow rate through the second micro-orifice can be increased by increasing the upstream pressure measured by P_1. All gas that is taken in with the slip stream, but is not part of the sample stream, is pumped out by the scroll pump. For the following tests, the carrier gas passed through the cryotrap bypass.

The effect of delivery pressure through the precision micro-orifice and changes in the flow rate were evaluated in order to characterize the RGA hydrogen detection system.

For the test in figure 3, 1% hydrogen in helium gas was flown in the carrier stream. The linear relationship between delivery pressure and hydrogen detector response in figure 3 shows that the pressure on the upstream side of the precision micro-orifice determines the gas flow into the vacuum. A four fold increase in the delivery pressure yielded a 28% increase in detected hydrogen. To first order, the detected signal was insensitive to the helium gas flow rate.

For the test summarized in table 1, only helium was flown in the sample stream. The hydrogen partial pressure detected by the RGA did not change with delivery pressure, but it did change slightly when the helium flow rate set by the MFCs increased. The very small hydrogen partial pressures indicate that the vacuum system is remarkably efficient at pumping out hydrogen.

Figure 4 illustrates the ratio between the partial pressures in figure 3 (with hydrogen flow) and table 1 (without hydrogen flow), and that ratio's dependence on flow rate and and delivery pressure. This shows the system's ability to distinguish different hydrogen concentrations under varying delivery pressures and flow rates. The system can differentiate between an absence of hydrogen and the presence of very small quantites of hydrogen. Also of note is that the ratio becomes less dependent on delivery pressure at higher flow rates. Operating at 150 sccm eliminates the detector's dependence on delivery pressure.

While this system allowed for predictable and precise measurments of hydrogen pressure, it took a very long time for all hydrogen to be pumped out the system once introduced, and the flow rate through the micro-orifices had to be recalculated every time the upstream pressure was changed. It also proved to be less sensitive than system 3.

System 3

The third system relies on permeation through a palladium/silver membrane. A schematic for this sampling approach can be seen in figure 5. In this system, a membrane separates the vacuum chamber from the carrier stream. The vacuum chamber draws gas from the carrier stream through the membrane, but the membrane is only permeable to atomic hydrogen. Molecular hydrogen dissociates on the membrane surface into atomic hydrogen which readily passes through the membrane and reforms as molecular hydrogen on the downstream side.**(3)** Most hydrogen in the carrier stream passes through the membrane. Helium and some hydrogen in the carrier stream leave through the exhaust system. Molecular hydrogen within the vacuum chamber on the downstream side is detected by ion gauge P. When heated above 180° C, the membrane diffusivity for hydrogen increases noticeably. In the present work, the membrane temperature was maintained between 250°C and 400°C. Temperatures below 400°C were used to ensure that the amount of hydrogen permeating into the vacuum system did not swamp the turbomolecular pump.

Figure 6 shows the relationship between hydrogen flow on the upstream side and the rate at which that hydrogen permeates into the vacuum chamber at various permeator temperatures. In figure 6, hydrogen mass throughput on the downstream side was calculated using the equation

$$\boldsymbol{\Phi_v = \frac{P}{\sum_{i=1}^{n} \frac{1}{C_i}} = PC_{net}}$$

where Φ_v is the mass throughput, P is the hydrogen partial pressure within the vacuum chamber in torr, n is the number of straight-tube sections (in series) connecting the membrane housing to the turbomolecular pump , C_i is the conductance of individual straight-tube sections (longer tubes have lower conductance), and C_{net} is the effective conductance of the entire vacuum system. For figure 6, the net conductance was simply the combined conductance of the turbomolecular and scroll pumps, 50 liters per second. As the temperature of the membrane increases, more hydrogen appears on the downstream side of the membrane. Not all hydrogen introduced to the membrane permeates through, indicating that the membrane is limiting hydrogen detection.

To determine how limiting the permeator is, the efficiency of the permeator at various temperatures was calculated and displayed in figure 7. The net conductance was found to be 26.1 liters per second. The hydrogen partial pressure was measured by a mass spectrometer and an ion gauge. At 400°C the Pd/Ag membrane transfers about 78% of the hydrogen available on the upstream side of the membrane, as shown in figure 7. Using this figure, the hydrogen flown in the system can be measured, even though some of it does not pass through the Pd/Ag membrane.

Characterization of the Cryotrap

Because system 3 (the permeation approach) had the highest sensitivity to hydrogen and was the most user friendly, it was chosen to detect hydrogen flowing through the cryotrap. The schematic for these tests is illustrated in figure 5.

The cryotrap was cooled with liquid nitrogen. The liquid nitrogen was flown through a stainless steel coil which was brazed to the stainless steel column containing the molecular sieve. The assembly was insulated to reduce heat loss to the surroundings. The column was cooled by thermal conduction once the cooling coil was filled with liquid nitrogen. The temperature of the cryotrap was monitored by thermocouples. Once the cryotrap reached temperatures around -180°C, helium gas was flown through the cryotrap bypass to establish a baseline reading on the mass spectrometer hydrogen detector. Once this baseline was established, the bypass was closed, the cryotrap was opened, and a hydrogen/helium carrier stream was flown through. This change in gas composition produced no change in the baseline, indicating that the molecular sieve was extracting all the hydrogen from the carrier stream. Once the column was filled to capacity, hydrogen would break through to the downstream side. At this point the hydrogen/helium flow was stopped and a pure helium stream initiated. The column was unloaded by raising the temperature of the column.

Figure 8 provides the partial pressure of hydrogen present downstream of the cryotrap as a function of time during the loading and unloading cycle of the cryotrap. Helium flowing at 150 sccm is co-mixed with hydrogen flowing at 40 sccm and introduced into the inlet of the cryotrap held at 93 K. Initially all the hydrogen is adsorbed on the cold molecular sieve. No hydrogen is detected downstream of the cryotrap, and the hydrogen partial pressure at the exhaust end of the cryotrap is at a background value. At 146 minutes hydrogen breaks through the cryotrap. A spike in the hydrogen partial pressure is observed followed by a steady although slightly declining hydrogen partial pressure. This curve suggests that initially a puff of hydrogen is released into the helium stream followed by a gradual release of hydrogen into the helium discharge approximately two orders of magnitude lower. The capacity of the column to hold hydrogen at 93 K before hydrogen appears at the outlet is 5.86 sL or equivalently 108.7 scc per gram of molecular sieve at 93 K (-180^{o}C).

At 209 minutes, the injection of hydrogen into the cryotrap inlet is stopped but the helium purge stream continues to flow at 150 sccm. Within a few seconds the hydrogen partial pressure in the exhaust stream is observed to decrease towards the original baseline value and remain at the low value until the cryotrap begins to warm up. Clearly the column can retain the captured hydrogen without releasing its contents to the helium purge stream provided the column remains cold.

At 210 minutes, the liquid nitrogen cooling to the coil is turned off but the coil does not warm up noticeably for an additional 13 minutes. At 233 minutes, the coil temperature reaches 127 K (-156^{o}C) and the hydrogen partial pressure is observed to increase above the baseline value. The majority of the hydrogen is released once the column reaches approximately 130 K (-140^{o}C). The remainder of the gas is released as the coil warms up beyond 170 K (-100^{o}C).

To understand if the initial spike observed at minute 146 in Figure 8 was an artifact of filling the coil to capacity, a second test was carried out in which the coil was filled to half capacity using the same loading conditions. The results are provided in Figure 9. At 85 min both the hydrogen and the liquid nitrogen flows were stopped. A spike similar to that observed in Figure 8 is observed moments after the hydrogen flow is turned off before the hydrogen partial pressure in the coil exhaust returns towards background. As the coil starts to warm up, the hydrogen partial pressure is observed to rise above its background value. This test establishes that the hydrogen partial pressure spike in the coil effluent is not a result of the cryotrap being charged to capacity.

Deuterium is naturally present in hydrogen gas at a concentration on the order of 150 ppm. To determine if D_2 is responsible for the spike observed in the two preceding tests, the experiment described in Figure 8 was repeated. However, in this test the residual gas analyzer (RGA) was set to measure the concentrations of three hydrogen isologues: H_2, HD and D_2. The results are illustrated in Figure 10. At 146 minutes hydrogen breaks through the column as before, once the column is fully loaded, and the characteristic spike is observed. However, increases in both HD and D_2 are also observed. The HD contribution is most likely a result of isotope scrambling of H_2 and D_2 to form HD as the two species permeate through the Pd/Ag membrane in the hydrogen detector. The D_2 partial pressure increase continues for an additional 30 minutes and then begins to decrease with time even after the hydrogen flow has been re-initiated at 319 minutes. The H_2 partial pressure increases to approximately the peak value of the initial spike and remains at that value even though hydrogen is being added at the coil entrance. Both H_2 and D_2 are being eluted from the coil at concentrations that do not depend on the inlet hydrogen/deuterium concentrations.

At 428 minutes the LN_2 cooling to the coil is turned off. Four minutes later, at 432 minutes, D_2 release from the coil increases rapidly to a reach an approximate steady state value until the column is emptied of D_2. The hydrogen concentration in the effluent drops, and at 428 minutes the coil has heated sufficiently to start the release of H_2 from the coil. All the D_2 is released in about 58 minutes. The bulk of the H_2 is released after 400 minutes. The details of this behavior will be the subject of future work.

Conclusions

Of the three hydrogen detection systems proposed for evaluating the performance of the cryotrap, the permeation system proved to be the most effective and feasible. It had a high degree of sensitivity and efficiency. The thermal conductivity detection system was difficult to implement due to the similar thermal conductivities of helium and 1% hydrogen in helium. The atmospheric sampling system, while workable, lacked the sensitivity of the permeation system.

Evaluation of the cryotrap with the permeation system revealed several interesting phenomena. Breakthrough is sudden and significant once the column reaches capacity. Hydrogen can be eluted from a full, cold column by continuously purging the column with helium. Deuterium can be separated from hydrogen by warming the column.

References

1. Shmayda, Walter. *Evaluation of Tritium Capture Systems*. 25th Symposium on Fusion Engineering. San Francisco, CA, USA. June 10-14 2013.
2. Jo, Aaron. *Hydrogen Isotope Separation Using Gas Chromatography*. 2012 Summer Research Program at the University of Rochester's Laboratory for Laser Energetics.
3. Yokogawa Corporation of America. *Hydrogen Permeation.* January 11, 2012

Acknowledgements

I would like to thank Dr. R.S. Craxton for allowing me to participate in this program. I would also like to thank Dr. Shmayda and Neil Redden for the incredible support they gave me, along with Andrew Boyce and Aaron Jo for the guidance they provided.

Figures

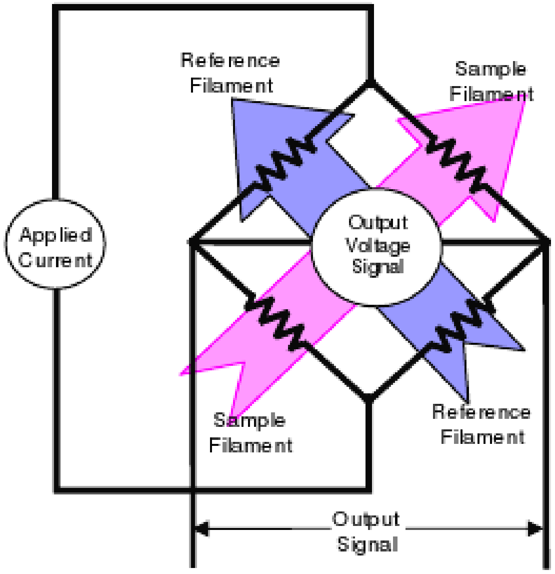

Figure 1. The Wheatstone bridge used for the thermal conductivity detector. The colored arrows represent the direction of gas flow. When the helium carrier gas flowing across the sample filaments includes hydrogen, the bridge becomes imbalanced, producing an output voltage signal.

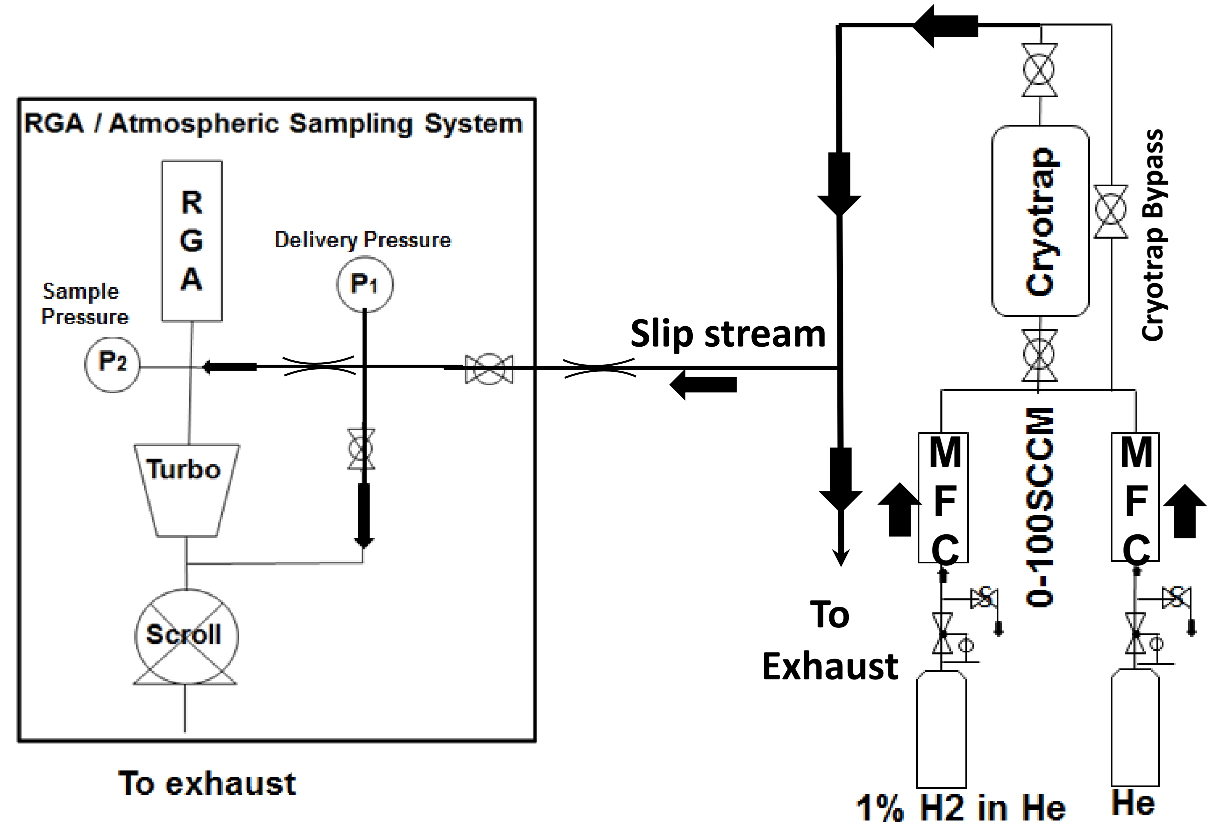

Figure 2. Schematic of the atmospheric sampling system with gas flow setup. Gas flowed through the cryotrap bypass for these tests. P_1 and P_2 represent ion gauges, which measure delivery pressure and sample pressure, respectively. "MFC"s are mass flow controllers, "RGA" is the residual gas analyzer with an RF-quadrupole mass spectrometer. The turbomolecular and scroll pumps draw gas through the system and create a vacuum.

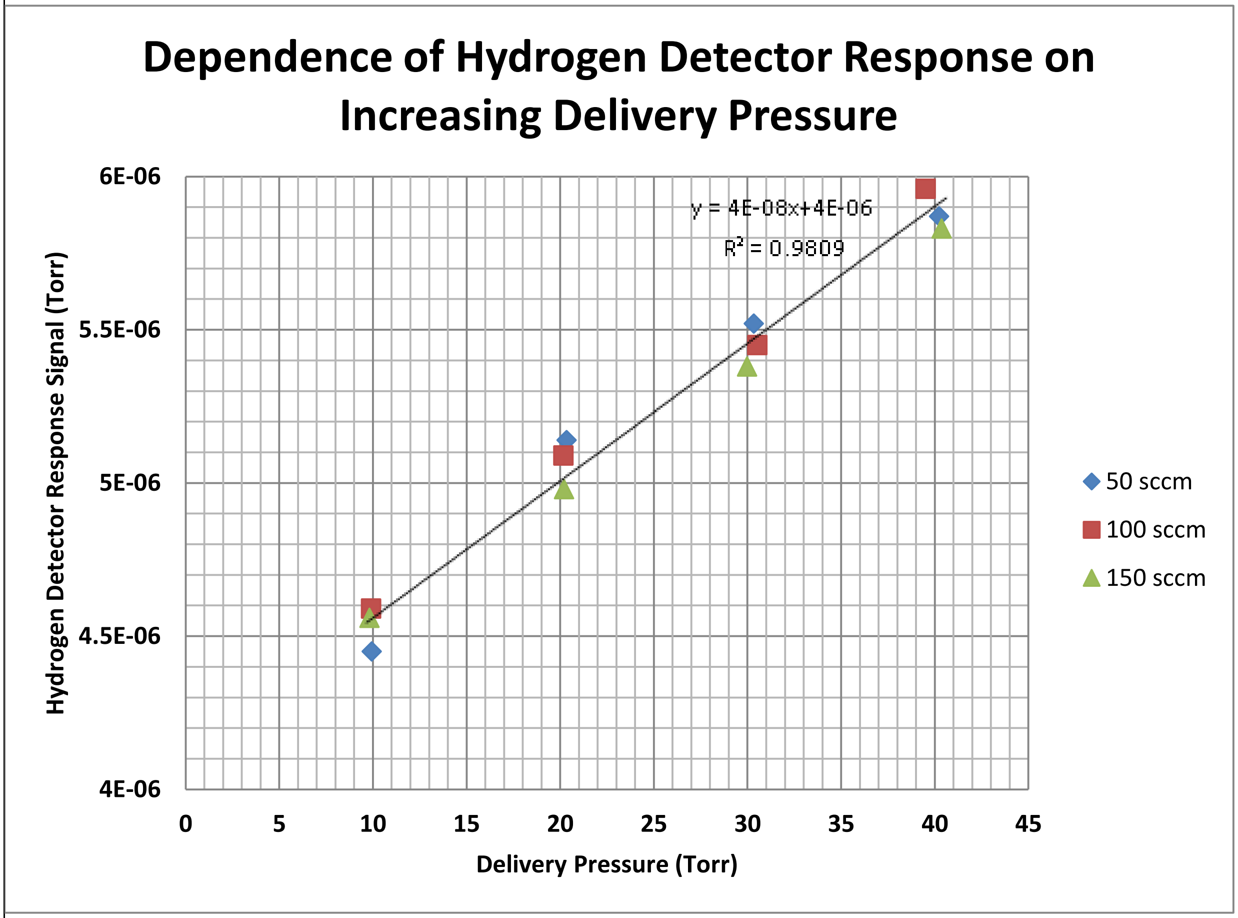

Figure 3. The dependence of the hydrogen detector response signal on increasing delivery pressure. The gas flow was 1% H_2 in He. The delivery pressure was measured by ion gauge P_1, and the detector response was measured by the RGA for flow rates from 50 to 150 sccm. Increasing the flow rate had no significant effect on detector response, so the different flow rates were given the same least-squares regression line.

He Flow rate (sccm)	Hydrogen Partial Pressure (Torr)
50	1.0E-06
100	5.2E-07
150	3.5E-07

Table 1. The hydrogen partial pressures detected by the RGA when only helium was flown in the sample stream. These pressures were slightly affected by changes in helium flow rate. Hydrogen partial pressures were independent of delivery pressure, hence the exclusion of delivery pressures from the table.

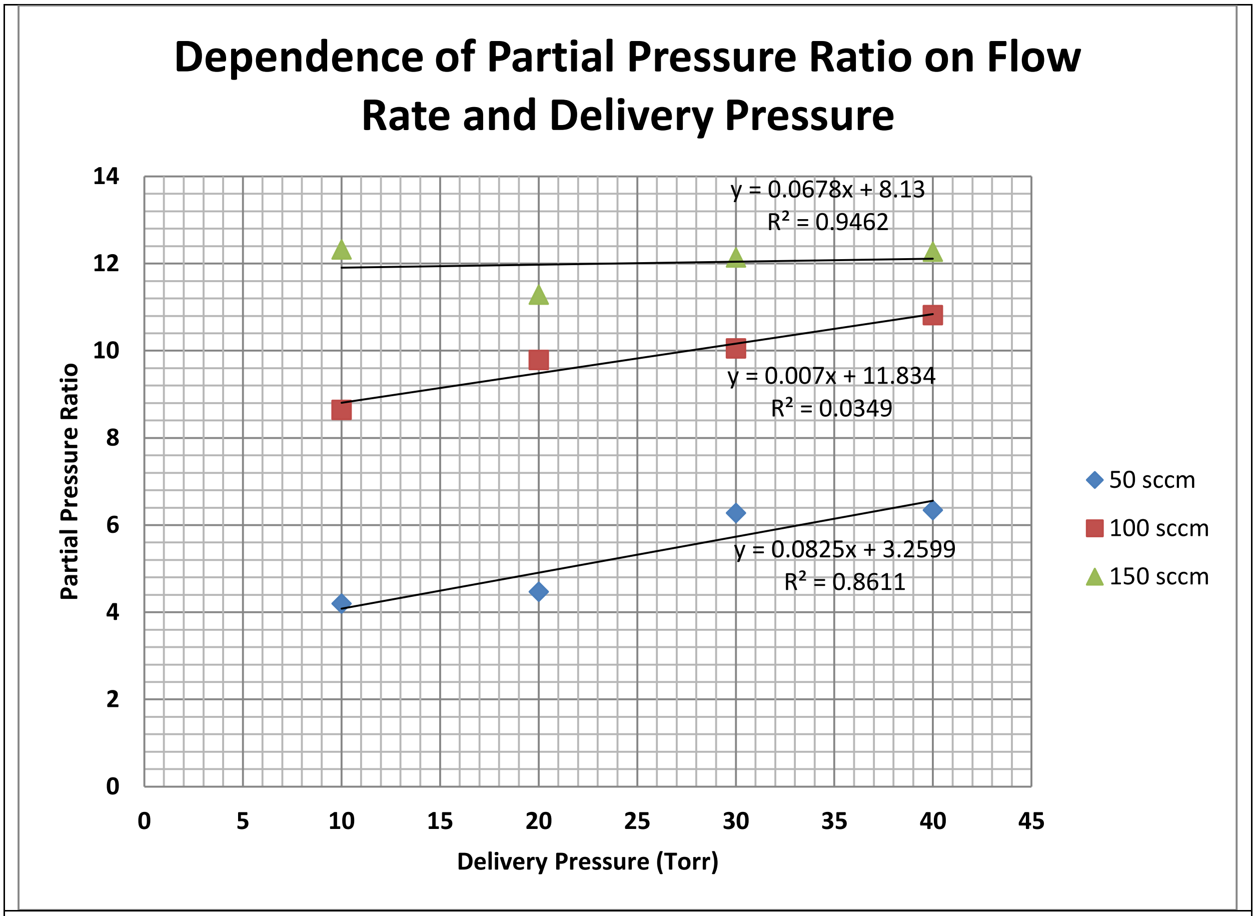

Figure 4. The dependence of the partial pressure ratio on flow rate and delivery pressure. The delivery pressure was measured by P_1. Partial pressure ratios are obtained by dividing figure 3 hydrogen partial pressures by table 1 hydrogen partial pressures of the same flow rate.

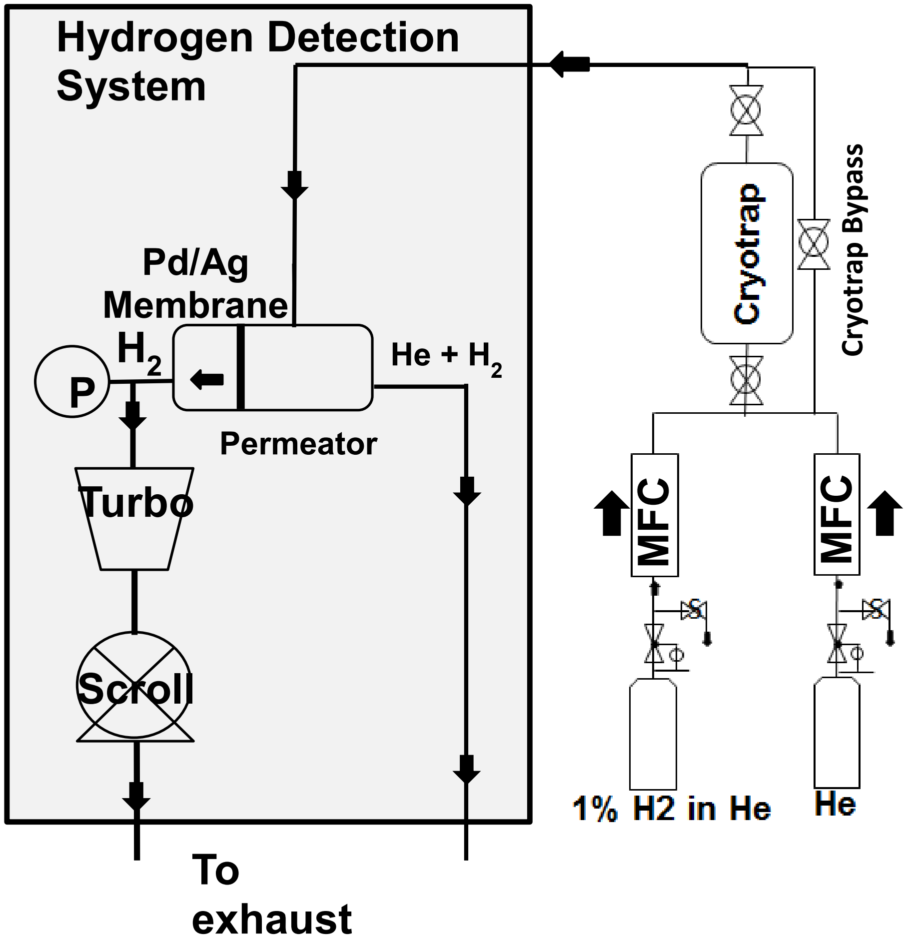

Figure 5. Schematic of the permeation sampling system. Most hydrogen permeated through the Pd/Ag membrane, while some hydrogen and all helium was immedately released as exhaust. The hydrogen that did permeate was detected by ion gauge P and pumped out by the turbomolecular pump backed by a scroll pump.

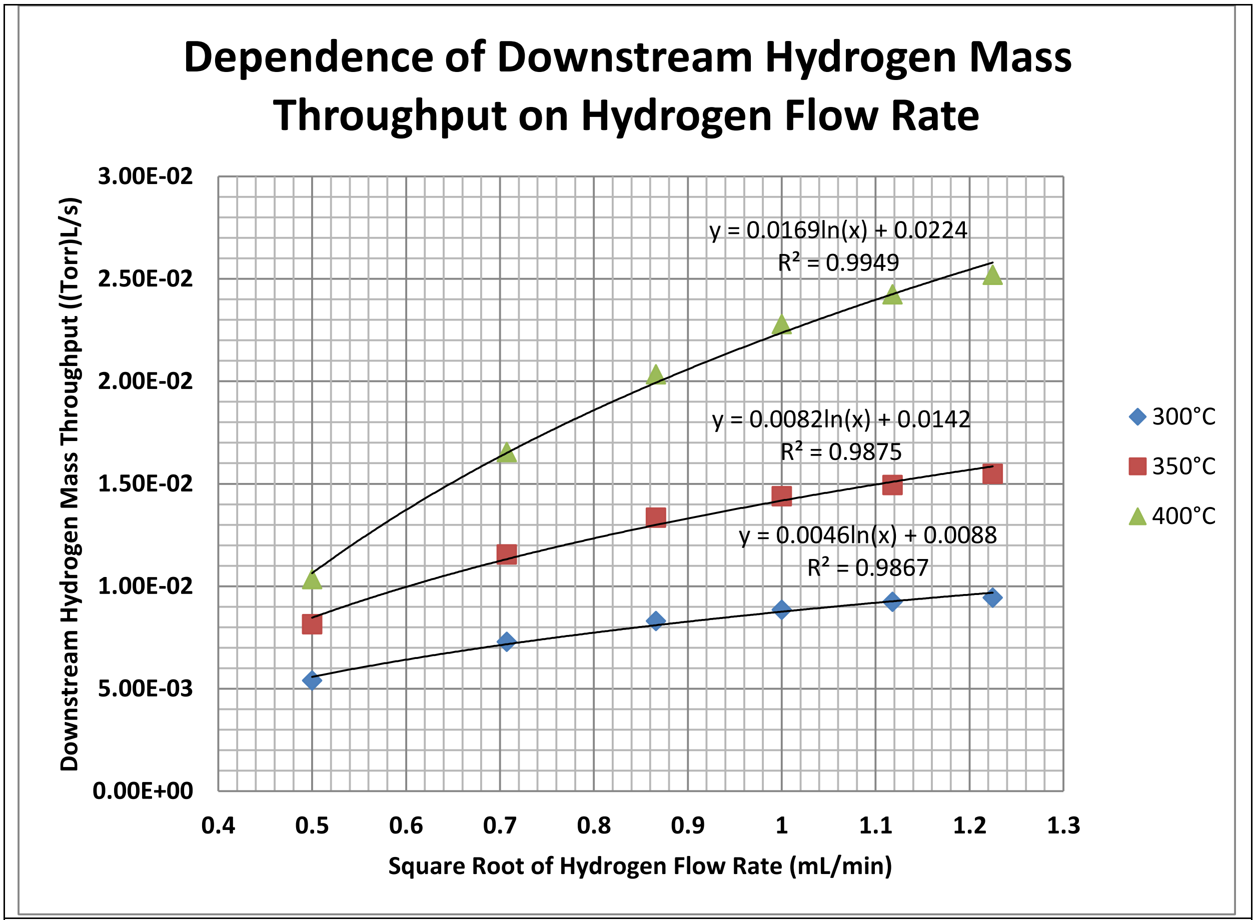

Figure 6. The dependence of downstream hydrogen mass throughput on the flow rate of hydrogen. Hydrogen mass throughput was calculated by multiplying the detected hydrogen partial pressure by the 50 L/s conductance.

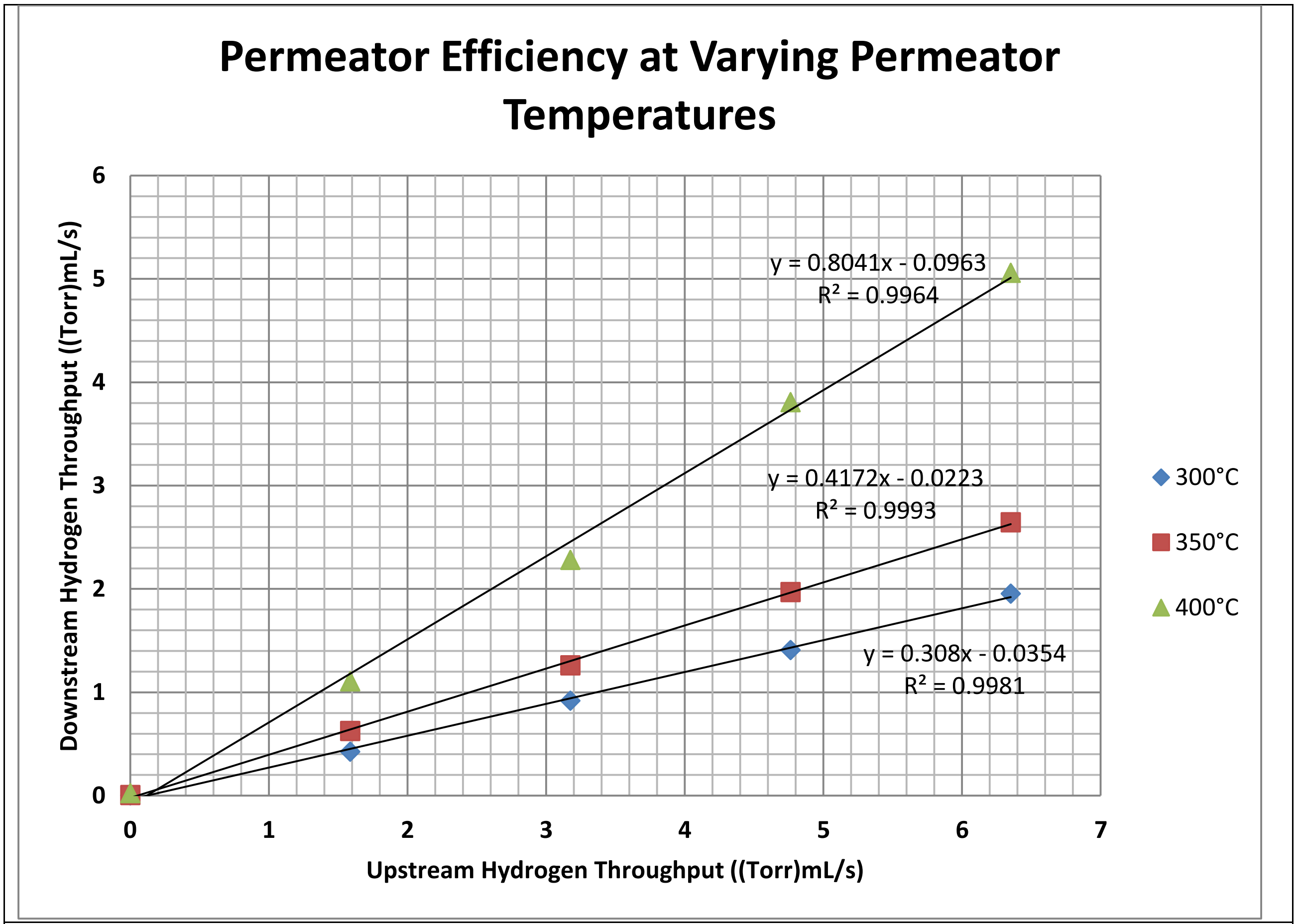

Figure 7. The downstream throughput of hydrogen relative to the upstream throughput at various temperatures. Permeator efficiency (the slope of the graph) is highest at higher membrane temperatures. He/H_2 carrier stream flows at 50 sccm. The hydrogen flow is controlled by a MFC, and hydrogen throughput (the rate at which hydrogen permeates into the vacuum chamber) is calculated based on measurements from the mass spectrometer.

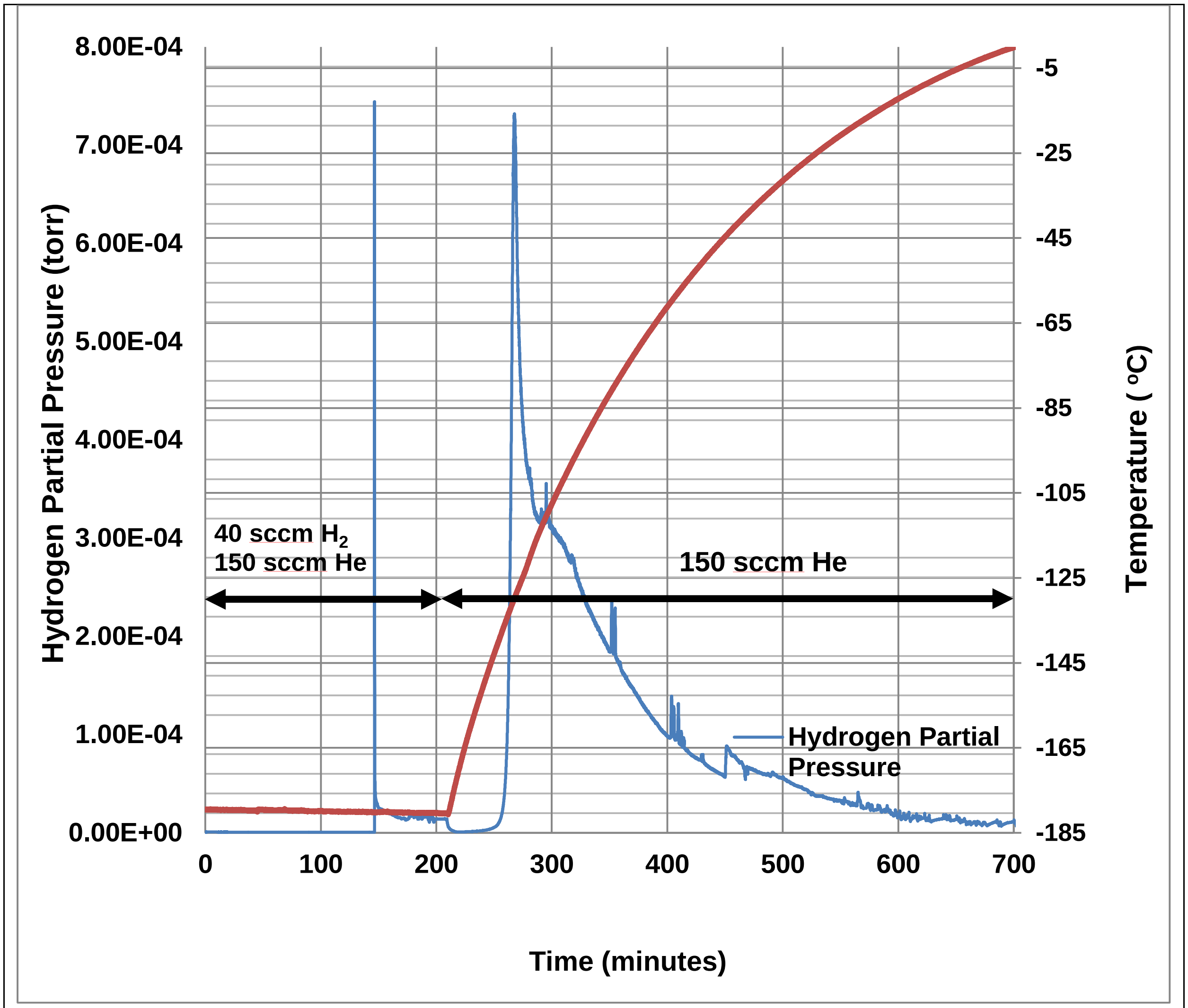

Figure 8. Partial pressure of hydrogen measured downstream of the permeator (the blue curve) as a function of time, illustrating a typical loading and unloading cycle for the cryotrap. The cryotrap reached its maximum hydrogen capacity at 146 minutes. The liquid nitrogen was valved off at 210 minutes. The permeator membrane was operated at 300° C for this experiment. Hydrogen charging the column was shut off at 209 minutes, and hydrogen stopped breaking through shortly after. Baseline partial pressure of 7E-7 torr. The red curve gives the temperature of the cryotrap as a function of time.

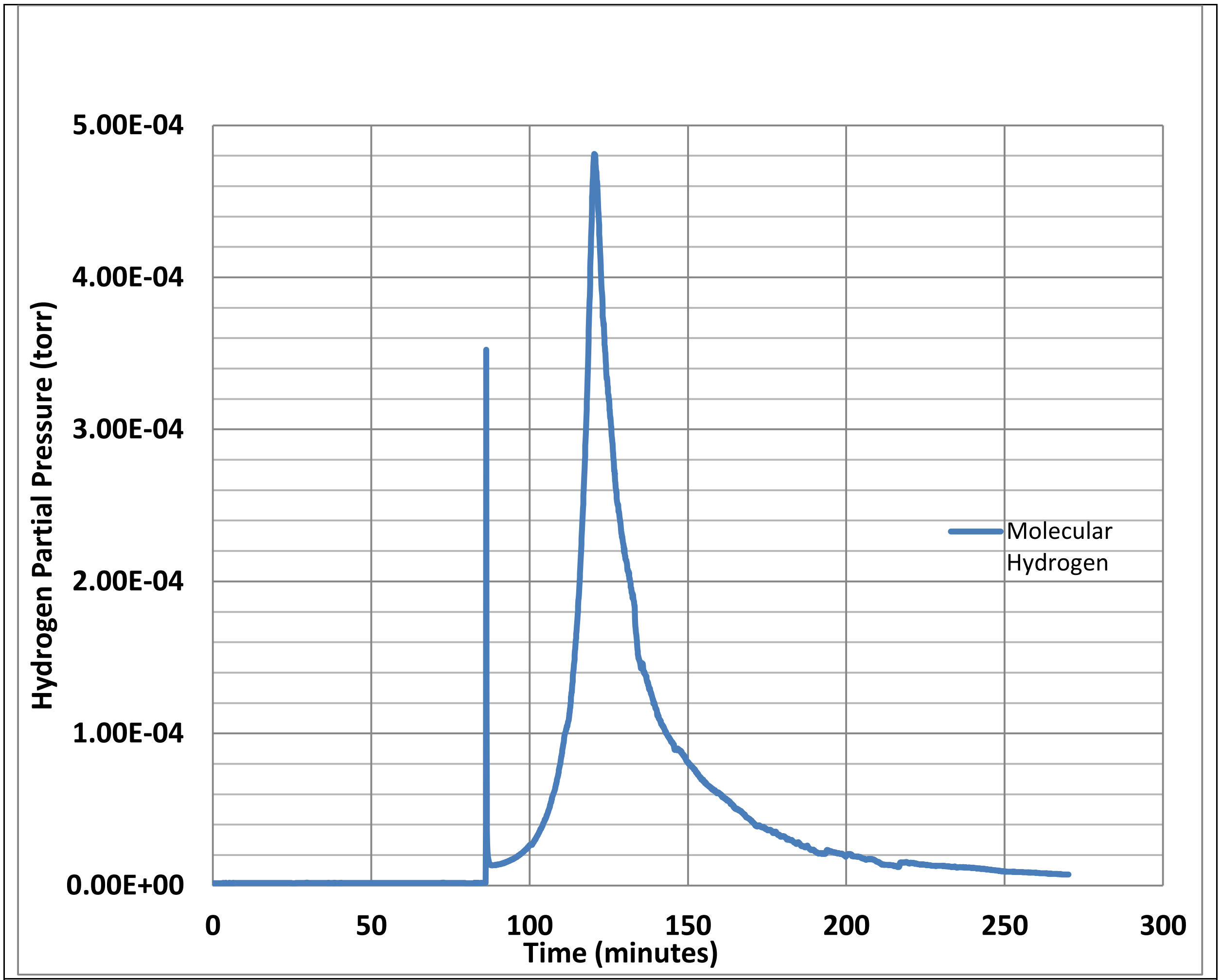

Figure 9. The same conditions as figure 8, but with the the 40 sccm hydrogen flow and liquid nitrogen flow stopped at 85 minutes. At this time, the molecular sieve was filled to half of its capacity. The permeator membrane was operated at 300ºC.

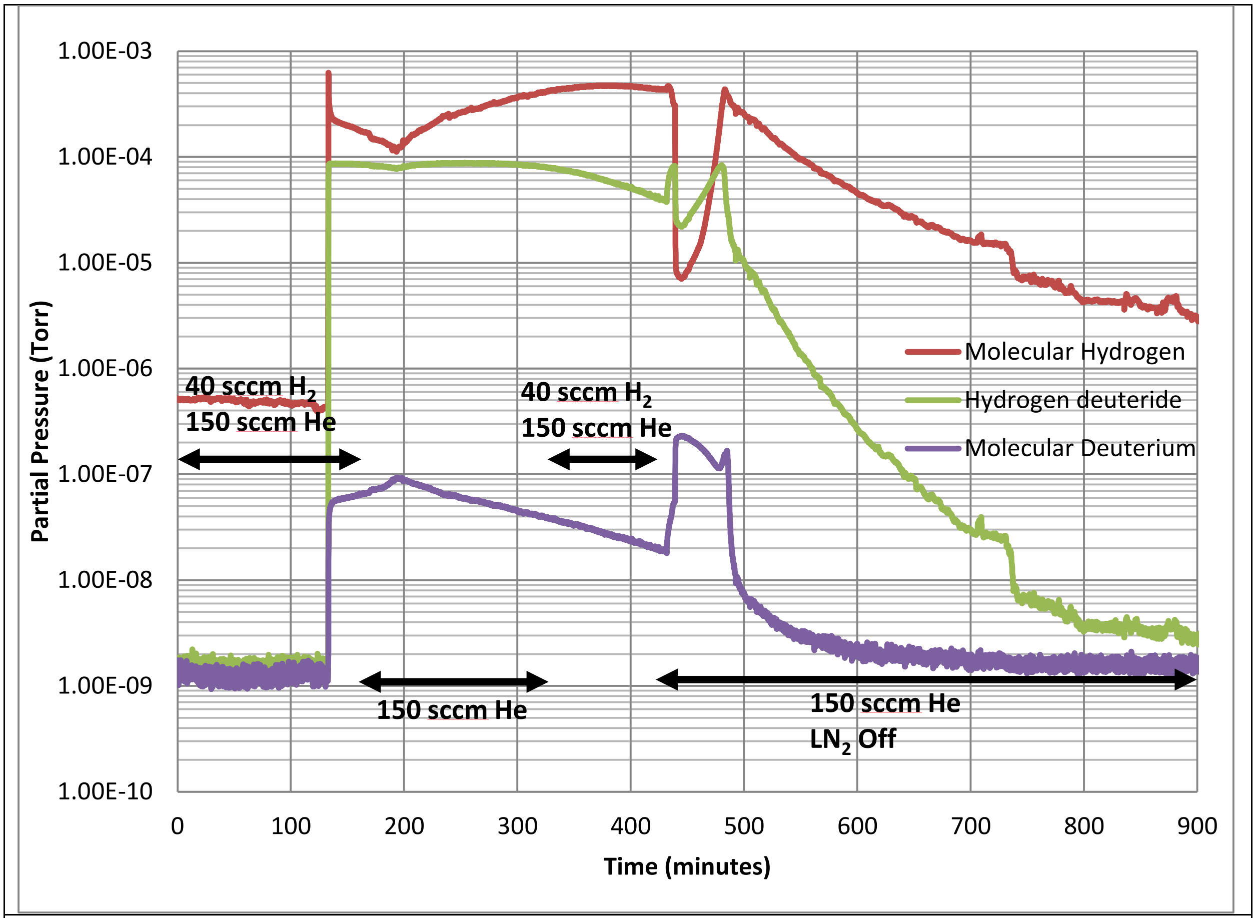

Figure 10. Partial pressures of molecular hydrogen, hydrogen-deuteride, and molecular deuterium measured as a function of time by an RGA in the vacuum chamber. The RGA detects all the hydrogen isologues: mass 2 is hydrogen, mass 3 is hydrogen deuteride, and mass 4 is deuterium. Only hydrogen and its isologues can permeate through the membrane, so the particles of masses 3 and 4 are unlikely to be contaminants of the same mass. Baseline hydrogen partial pressure is about 4.7E-7 torr. H_2 was turned off at 166 minutes and on again at 319 minutes, before being turned off for the final time at 428 minutes. Temperature increased at the same rate as in figure 8 once liquid N_2 was turned off at 428 minutes.